POLITECNICO DI TORINO
Repository ISTITUZIONALE

Voltage control in low voltage grids: A comparison between the use of distributed photovoltaic converters or centralized devices

(Article begins on next page)

20 April 2024

Voltage Control in Low Voltage Grids: a Comparison between the Use of Distributed Photovoltaic Converters or Centralized Devices

Alessandro Ciocia, Gianfranco Chicco, Paolo Di Leo, Marco Gai, Andrea Mazza, Filippo Spertino
Dipartimento Energia "Galileo Ferraris"
Politecnico di Torino
Corso Duca degli Abruzzi 24, 10129 Torino, Italy
{alessandro.ciocia, gianfranco.chicco, paolo.dileo, andrea.mazza, filippo.spertino}@polito.it;

Nouredine Hadj-Said
G2Elab
Grenoble INP
38402 Saint-Martin-d'Hères, Grenoble, France
nouredine.hadjsaid@g2elab.grenoble-inp.fr

Abstract— **In this paper, three solutions for the control of voltage in Low Voltage (LV) grids with high photovoltaic (PV) penetration are simulated and compared. The first solution corresponds to the use of distributed PV converters to control voltage in their connection points. In other cases, a centralized control is performed, by using a Static Var Compensator or a transformer with On Load Tap Changer installed inside the MV/LV substation. Benefits on voltage profiles and reduction of losses are shown through simulations carried out on a real grid. The consumption and PV generation profiles come from accurate measurements performed in apartment and office buildings with 1-second time step.**

Keywords— Grid integration, photovoltaic system, voltage control, low voltage grid, reactive power, static var compensator;

I. INTRODUCTION

In recent years, the penetration of PhotoVoltaic (PV) systems has been increased: at the end of 2015, the worldwide installed power (mostly grid-connected) reached 196 GW, with an increase of 56 GW with respect to 2013 [1][2]. A considerable amount of PV generators is connected to Low Voltage (LV) grids. High PV penetration levels in LV grids may cause technical issues, such as voltage rise, the increase of harmonic content, and unbalance [3]. The effect of the deterioration of voltage profiles along the lines ranges from the accidental disconnection of the interface protection systems of the PV DC-AC converter to stability problems in the grid. Thus, Distribution Network Operators (DNOs) have to consider new solutions to guarantee normal operation and satisfy quality standards. For example, the Standard EN 50160 sets out power quality requirements [4]; regarding the Root Mean Square (RMS) value of the voltage, it cannot exceed ±10% of its nominal value (in LV grids V_{nom}=230/400 V).

In some countries, such as Germany, some MV/LV transformers have been replaced with new devices equipped with an On Load Tap Changer (OLTC). The effectiveness of these devices in case of high PV penetration is actually under study: different works demonstrate the presence of benefits on voltage control [5][6][7]. In other cases, it is established that the related increase of renewable hosting capacity is modest or non-existent [8]. In addition, the widespread use of OLTC is expensive, because it requires the replacements of old transformers and high O&M costs (depending on the number of tap changes occurring during time). Economic aspects still have to be carefully estimated, and techniques to optimize (from both economic and technical points of view) the number of tap changes are currently under study [9].

Instead of replacing old transformers, another solution for voltage control is the installation of a Static Var Compensator (SVC), which has fast operation and good reliability. Thanks to power thyristors, this device presents many advantages with respect to an OLTC, in particular, high reaction speed and low maintenance. The SVC does not have mechanical commutation problems (sudden voltage variations and transient perturbations); it is a mature and cheap technology and has very low contribution to the short-circuit power. In addition, it is technically possible to install a centralized device (as in case of an OLTC) or several distributed SVCs in the weakest points of the grid. In [10], a selection of the optimal SVC location is defined to maximize the PV penetration in the grid.

Another method to mitigate the negative effect of power injection on voltage profiles is the control of reactive power performed by AC-DC converters of PV systems. Generally, PV plants work with unity power factor, and over-voltages are reduced by limiting

the active power injected into the grid. Nevertheless, new regulations work in the direction of making the PV converters "active" components that provide ancillary services. For example, in Italy, the Standard CEI 0–21 [11] requires that PV inverters manage reactive power to control the voltage in their Connection Points (CPs), when the injection of active power is higher than the defined limits. In [12], voltage and frequency control algorithms are developed according to the prescriptions of [11]. The algorithms allow studying the impact of this control on the distribution network and on PV systems.

In the present work, the three above described solutions for voltage control in LV grids with a high PV penetration, namely, the use of distributed PV converters or centralized devices (a SVC or an OLTC), are simulated and compared.

In the first case, only the distributed PV inverter performs voltage control, and there is no centralized management. The converters continuously check the voltage at their CPs and exchange reactive power to stabilize it. With respect to the Standard CEI 0–21, the voltage band in which the inverters have to work is slightly modified to obtain higher benefits on voltage profiles.

In the second case, a centralized control is evaluated by simulation of the operation of an SVC installed inside the MV/LV substation. The SVC stabilizes the voltage at the LV bus of the transformer, and it is supposed that this device does not know the voltage levels in the other nodes of the LV grid. The third case study corresponds to the use of an OLTC: as in the case of the SVC, there is no data communication between the substation and the other nodes. In the last two cases, only a centralized device is used (a SVC or an OLTC) and the PV inverters do not control the voltage in their CPs.

The real LV grid used for the simulation is located in an Italian city, and the loads correspond to apartment and office buildings. Consumption and PV generation profiles are collected from accurate measurements performed with 1-second time step.

The next sections of this paper are organized as follows: in Section II a description of the system is presented, with details related to the grid configuration and its main components (e.g., lines, transformer, loads and distributed generators). The power flow simulation is introduced in Section III. In Section IV the devices and methods used for voltage control are presented. In Section V the simulation results at different penetration of PV generation are illustrated and discussed.

II. SYSTEM ARCHITECTURE

A. LV grid

The analyzed LV grid is part of the three-phase network of an Italian city. As shown in Fig. 1, it consists of 20 lines and 21 nodes (of which the slack node #0 is the MV bus of the MV/LV substation).
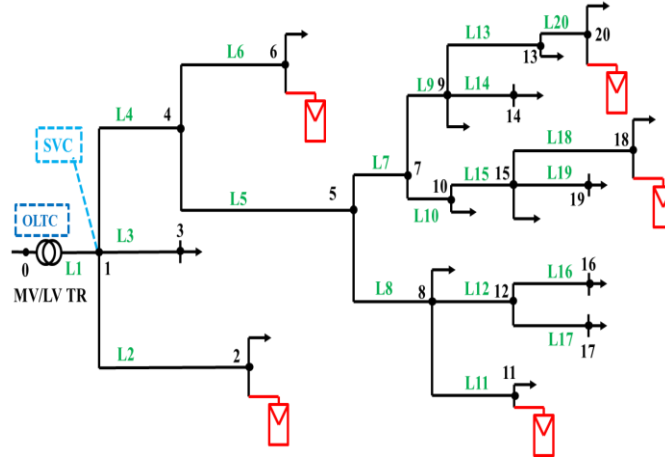

Fig. 1. LV grid under study

The system has grounded neutral and lines with three-pole underground cables, except for the first overhead cables in proximity of the transformer (lines #L2, #L3 and #L4). In addition, Fig. 1 shows the position of the PV generators in the grid, and the possible connection of an SVC or an OLTC (dashed boxes).

In all the lines, the resistive component of the cables prevails over the inductive one. In case of the worst CP (node #18), the total resistance of lines is ≈121 mΩ, while the total reactance is ≈28 mΩ (transformer excluded). For the solution of the load flow problem, the lines have been modeled with an equivalent system in which the capacitive parameters are neglected, due to short lengths (the longest line measures ≈ 81 m).

Since the loads in the simulation are considered at the buildings CPs (i.e., each load profile corresponds to the aggregation of different apartments and/or offices), it is assumed that the system is symmetrical and balanced. In this way, the simulation can be performed considering an equivalent single-phase model limited only to the positive sequence.

B. Transformer

The transformer is not equipped with devices for the voltage control: the voltage level is seasonally changed thanks to an off-load tap change. It is a three-phase transformer 20kV/400V with a rated power $S_{rated,tr} = 400$ kVA, a nominal current $I_n = 577$ A, a short-circuit impedance $Z_{sc} \approx 24$ mΩ, and a short circuit power at 75°C $P_{SC\_75°C} = 4.7$ kW. The transformer is represented with a pi-model, neglecting the shunt parameters. The series impedance is calculated starting from the transformer datasheet; in the model of the network, it corresponds to the impedance of line #L1.

C. Load and generation profiles

Two types of loads are present in the simulations: apartment and office buildings. Fig. 2 shows an example of PV generation (a day with high solar irradiance) and apartment and office active consumption profiles (reactive consumption is omitted in the figure). In case of apartments, the highest consumption peak generally occurs in the evening between 7 and 10 pm, when people come back from work. Another peak occurs in the morning between 7 and 9 am, before working activities. Thus, the consumption profile of apartments does not well match the generation profile of PV systems and this difference can be one of the reasons of the deterioration of voltage profiles.

Nevertheless, as shown in Fig. 2, if one or more family members are at home during the day, the consumption can be high also at midday (the load profile in Fig. 2 refers to a single apartment). Consumption peaks can be attributed to household appliances converting electricity into heat (e.g. hairdryer, iron, boiler or oven) or mechanical work (e.g. washing machine).

In case of office buildings, the PV power production matches very well the loads [13], as office activities prevail in the middle of the day. As shown in Fig. 2, the employees come in mainly at 8-9 am and leave at 6 pm.
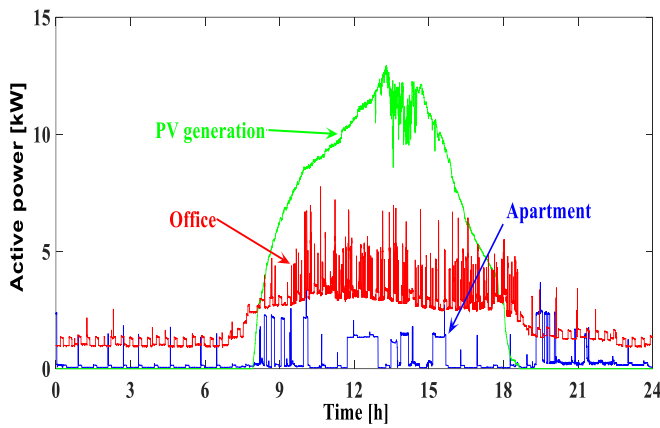

Fig. 2. An example of measured loads and generation profiles.

In order to measure actual power flows, the Data Acquisition (DAQ) System described in [14] has been used. It is periodically calibrated and made of a personal computer and a data acquisition device, equipped with one A/D converter (successive approximation, 16 bit-resolution and maximum sampling rate of 1.25 MSa/s) and multiplexer for eight differential channels. Voltage and current measurements are performed by 3 voltage differential probes (peak values of ±1000 V_{pk}) and 3 Hall effect current probes (for DC/AC, peak values of ±200–2000 A_{pk}), respectively.

After measurements, the production profiles of the tested converters have been checked in order to verify their correct operation. As shown in Fig. 3, the power quality towards the grid is acceptable. The total harmonic distortion of current THD_I and voltage THD_V are lower than 5%, and the power factor is PF ≈ 1 close to full load [14].
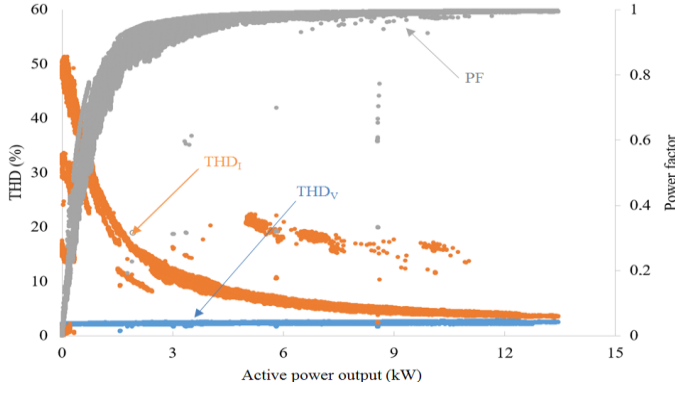
Fig. 3. Power factor and total harmonic distortion of current/voltage

III. POWER FLOW SOLUTION

In the power flow calculation, the key point is the determination of voltage values, in magnitude and phase, in each node of the network. In the present work, the radial network under analysis has a symmetrical and balanced configuration, therefore, the Backward Forward Sweep (BFS) technique has been used. At the end of each iteration m, the maximum voltage deviation is calculated in every node (N is the number of nodes in the network, slack node excluded), with respect to the previous iteration. In particular, if the deviation is below a threshold ε defined a priori, the procedure is stopped, and the voltages converge to the final values:

$$\max_i \left\{ \frac{\overline{V}_i^{(m)} - \overline{V}_i^{(m-1)}}{\overline{V}_i^{(m-1)}} \right\} < e \qquad \text{for } i = 1, ..., N \qquad (1)$$

where $\overline{V}_i^{(m)}$ is the voltage calculate in node i at iteration m, while $\overline{V}_i^{(m-1)}$ is the same value calculated at the previous iteration m-1.

IV. SOLUTIONS FOR VOLTAGE CONTROL

A. Voltage control performed by distributed PV converters

The voltage control can be performed by distributed PV converters, in order to stabilize voltage in their respective CPs, without communication with each other or with a centralized unit. Generally, the majority of the devices manage reactive power in the same direction, due to external conditions. For example, during a sunny Sunday, the external conditions correspond to high productions and low loads in the entire feeder, which obviously means a global high voltage level.

In order to handle this issue, it would be possible to act either on the active power (taking into account the significant resistive nature of the lines) or on the reactive power. With the idea of using all the active power generated locally (to maximize the impact of the generation from renewable sources), the voltage control is attempted by managing the reactive power available from the converters inside their capability limits. The extent of the reactive power managed by the converters also depends on the power flows and of the position of the converters in the grid. Thereby, the behavior of each device can change with respect to the general trend. This behavior is intuitively like to a school of fish, in which all the fishes swim together in the same direction, but each of them can move away for food (the same basic idea is used for the particle swarm optimization method [15][16]). In case of PV converters, each one manages reactive power to stabilize its CP and can affect voltage in other CPs (making them even worse). This is the limitation of a system without communication between the distributed devices. As described in next paragraphs, the procedure to simulate the system is developed also to take into account this aspect and evaluate its effects.

The first step of the procedure (STEP#1 in Fig. 3) corresponds to the power flow solution without voltage adjustment. In this way, the voltage levels are defined in all the nodes of the grid, while active power injections are inputs of the simulation.

The second step of the procedure (STEP#2) uses the voltage levels calculated at STEP#1 and the active power injections P_{out} to identify which converters are involved in the voltage control. According to the Italian Standard CEI 0–21 [11], a PV converter with rated power higher than $\approx$11 kVA participates in voltage control only if the output active power $P_{out,PV}$ exceeds 20% of the rated value $S_{rated,PV}$ and the voltage lies within defined ranges ($0.9 < V < 0.92$ or $1.08 < V < 1.1$ p.u.). Outside the admitted voltage range 0.9–1.1 p.u., the converter has to follow other rules defined in the abovementioned standard. In the present work, the Standard CEI 0-21 is respected with more rigorous requirements concerning the voltage ranges in which converters have to work. The device has

to reach a *target voltage range* ($V_{target,min}$–$V_{target,max}$) close to the unit value (0.995–1.005); the reason is to estimate the potential of this technique in stricter conditions.

After the identification of the converters involved in voltage control, the maximum level of reactive power $Q_{max,n}(t)$, that the device (installed in node N) can provide, is calculated (STEP#3). The Standard [11] requires the respect of a triangular capability curve, so that the Power Factor (PF) never decreases below the limit $PF_{min} = 0.9$. Thus, the maximum available reactive power is calculated as:

$$Q_{max,n}(t) = \sqrt{S^2_{rated,PV} - P^2_{out,n}(t)}$$

$$\text{with } P_{out,n}(t) \geq 0.9 \times S_{rated,PV}(t) \qquad (2)$$

$$Q_{max,n}(t) = P_{out,n}(t) \times \tan(\cos^{-1}(0.9))$$

$$\text{with } P_{out,n}(t) < 0.9 \times S_{rated,PV}(t) \qquad (3)$$

Then, in STEP#4, the needed amount of reactive power to control voltage is calculated by an algorithm based on the *perturb and observe* technique. It means that, for each time step, the corresponding subroutine works. At each iteration of this subroutine, first, the reactive power is varied by a constant amount, then, the BFS technique is used to solve the new power flow. The voltage level in the CPs of each working converter is compared with the target voltage range. In this way, it is defined if it will be necessary to increase or decrease the reactive power injection during next step. The procedure is repeated until two criteria are respected:

1. the target voltage range is reached in the CPs of the working converter;

2. the reactive power limit of the converter has been already reached.

This calculation is performed for all the PV converters involved in voltage control. The list of working converters is uploaded at each iteration, because the work of a device could interfere with the operation of the others. For example, in the case of a feeder with two PV generators (GEN#A and GEN#B), the one connected at the end of the line (GEN#B) could suffer a low voltage level. For this reason, it provides capacitive power and the voltage level of the whole feeder increases. In the worst case, GEN#A could be affected by a high voltage and start working to compensate it. In a better case, the operation of GEN#A could stabilize voltage in the whole feeder such that the operation of GEN#B is not necessary anymore.

Finally, at the end of the subroutine, the contribution of all the converters is defined and the power flow at next time step is solved. The procedure is shown in the flowchart in Fig. 4.
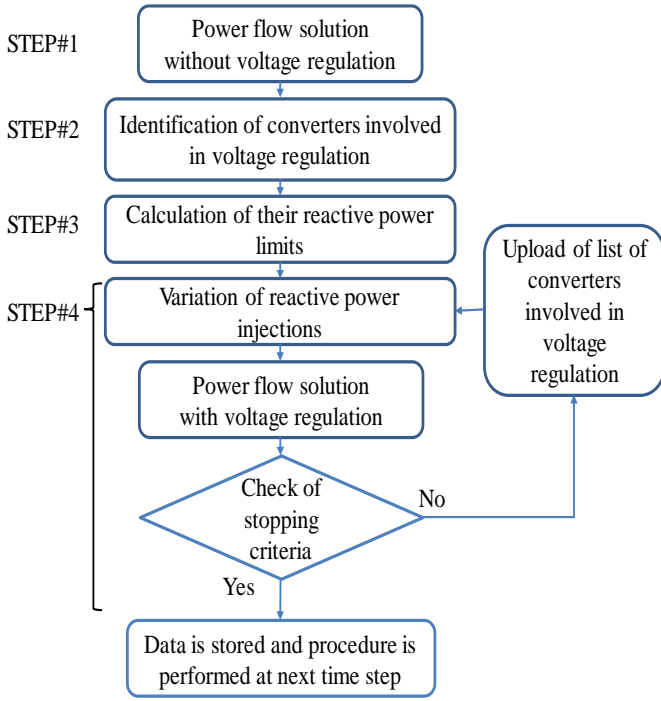
Fig. 4. Procedure for simulation of voltage control by distributed converters.

B. Voltage control performed by a centralized SVC

A SVC is a device able to control the voltage absorbing or injecting reactive power in the node where is installed thanks to the use of thyristor valves. There are several typologies, different for the operation and the used components. In the present work, a TSC-TCR (Thyristor Switched-Capacitor, Thyristor-Controlled Reactor) is simulated. Regarding the sizing of the components, the limit on the maximum reactive power supplied $Q_{SVC,min}$ is -30 kvar, while inductors can absorb $Q_{SVC,max} = 10$ kvar. These values were chosen by analyzing the overall load profile.

In the present work, the SVC is installed inside the MV/LV substation, with the purpose to evaluate the performance of a compact and relatively cheap device. In this way, it will be installed in a preexistent structure, property of the distribution operator, which can easily manage its operation. In addition, the replacement of the old transformer is not required, unlike in case of the installation of a new OLTC. As in the other cases, no communication systems with other parts of the grid are present; thus, voltage adjustment is possible only by measuring the voltage level at the LV side of the transformer. In this way, it is not possible to act on the individual nodes in the feeders.

Regarding the operation of the SVC, the simulation procedure is similar to the one used for the distributed converters. The first step (STEP#α) consists of the power flow solution without voltage adjustment: the voltage level is defined in all the nodes of the grid, but only that one corresponding to the LV side of the transformer is used for voltage control. This value is compared to the target voltage range (STEP#β): if an adjustment is needed, then the *perturb and observe* technique is used in a subroutine to vary the reactive injection (STEP#γ). At each iteration, the reactive power is varied by a constant amount, then, the BFS technique is used to solve the new power flow. The procedure is repeated until the target voltage range is reached or the maximum reactive power ($Q_{SVC,min}$ or $Q_{SVC,max}$) is provided. Finally, at the end of the procedure, the reactive power injection from the SVC is obtained and the power flow at next time step is solved. The procedure is shown in the flowchart in Fig. 5.
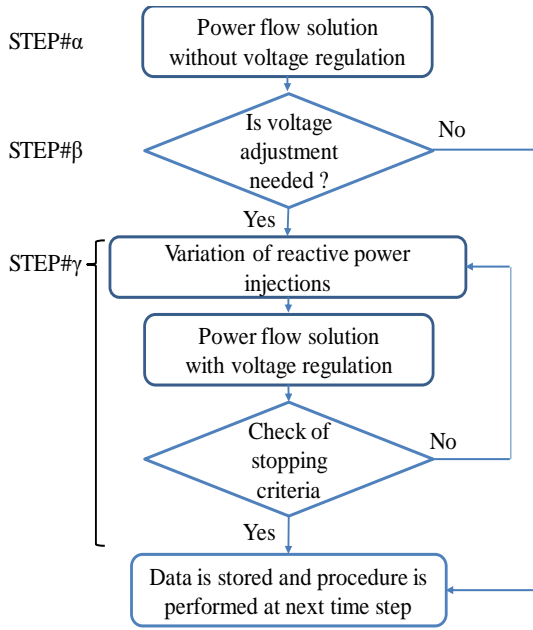
Fig. 5.   Procedure for simulation of voltage control by an SVC.

C. Voltage control performed by an OLTC

The OLTCs are devices able to vary the voltage level of a transformer without the need to switch off the loads. There are different types, which differ for the components used (mechanical or electronic tap changers). In every case, the replacement of the old transformer (equipped with an off load tap changer) is required. The simulated device is characterized by voltage step of 1.25% of nominal value and seven tap positions (-3,…,0,…,+3) corresponding to a voltage controlled in the range 0.9625–1.0375 p.u. The minimum admitted time between two taps, used as an input in the simulations, is a key-point from an economic point of view. In case of a widespread use of OLTCs in LV grids, in order to reduce overall O&M costs, the number of daily taps have to be reduced. In the present work, the device is assumed to change tap four times per day at most.

Regarding the OLTC operation, the simulation procedure is described by the following steps. At first (STEP#A in Fig. 6) the power flow solution is performed with the pre-existent tap position. The resulting voltage corresponding to the LV side of the transformer is used for voltage control in STEP#B: if it is inside the admitted range, the tap change is not necessary and the grid is analyzed at the next time step. Otherwise, the procedure continues in STEP#C with the check of the time elapsed from the last tap change. If the minimum admitted time between two taps is passed, the voltage control can be performed by the OLTC. The new position is higher than the previous one, if the voltage (the average value during the time after the last tap change) is lower than target voltage range and vice versa for higher voltage (defined in STEP#D). STEP#E corresponds to the power flow solution performed with the new tap position. Obviously, if the maximum or the minimum tap position has been already reached, it will not be possible to carry out further tap changes in the same direction. The procedure is shown in the flowchart in Fig. 6.
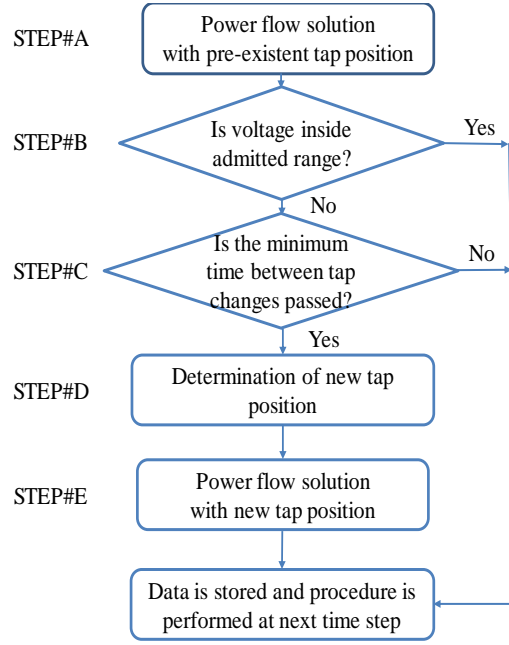
Fig. 6. Procedure for simulation of voltage control by an OLTC.

V. SIMULATION RESULTS

The simulations are performed at different levels of PV penetration in the grid α_{CP}, defined as the ratio between the daily peak power produced by distributed generators P_{PV} and the peak load during the day P_L. In the present work, α_{CP} will range from 25% to 75%.

Fig. 7 shows the evolution in time of the voltage profile at node #18 (it corresponds to the CP of the PV plant with the highest nominal power $P_{PV} \approx 65$ kVA) in case of high PV penetration $\alpha_{CP} = 75\%$. In this case, the use of a centralized SVC is the best solution: thanks to this device, voltage ranges from $V_{min} \approx 0.93$ to $V_{max} \approx 1.04$ p.u. during the whole day, while in the reference case without control the voltage range is 0.91–1.04 p.u.

Additionally, the PV inverters provide a good control, nevertheless their operation is limited, because it is linked to active power injection and they cannot work during evening and night, according with [11]. Thus, the minimum voltage level corresponds to that one of the reference case without control ($V_{min} \approx 0.91$ p.u.). On the contrary, an SVC, originally installed to control voltage during light hours, can be used to increase the voltage also during the evening, when there is load peak in apartment buildings.
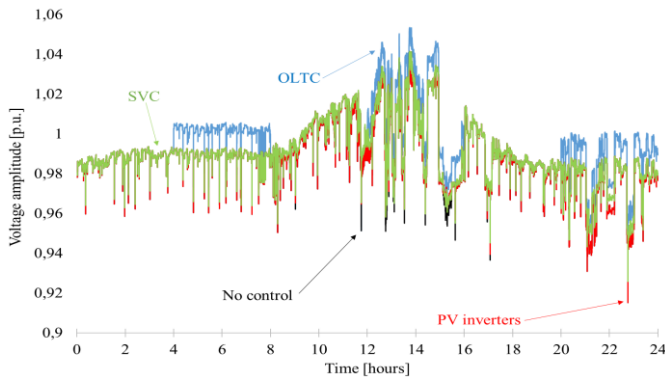

Fig. 7. Voltage profiles with different controls; node #18, α_{CP}=75%.

TABLE I. RESULTS OF SIMULATIONS WITH HIGH PV PENETRATION

α_{CP}=75%		Voltage amplitude (p.u.)		
		Node #1	Node #10	Node #18
No control	V_{max}	1.001	1.027	1.042
	V_{min}	0.983	0.935	0.915

αCP=75%		Voltage amplitude (p.u.)		
		Node #1	Node #10	Node #18
	V_{average}	0.995	0.990	0.990
Distributed PV converters	V_{max}	1.000	1.021	1.034
	V_{min}	0.984	0.935	0.915
	V_{average}	0.995	0.990	0.990
OLTC	V_{max}	1.013	1.039	1.054
	V_{min}	0.983	0.949	0.929
	V_{average}	1.001	0.997	0.997
SVC	V_{max}	1.001	1.027	1.042
	V_{min}	0.995	0.946	0.926
	V_{average}	0.996	0.991	0.991

An OLTC can follow the evolution of the load during of the day, if the tap position is continuously changed. In this work, in order to reduce the wear of the device, the number of tap changes is low (max 4 per day). Thus, the performance of this device is low. In addition, in case of high variability of PV generation, the stress due to the voltage level can increase (in Fig. 7, $V_{\text{max}} \approx 1.05$), with respect to the case without control.

Table I shows the results of the simulations with high PV penetration $\alpha_{CP} = 75\%$ in terms of maximum, minimum and average voltage during the day. Node #1 corresponds to the low voltage side of the transformer: due to its low impedance, the voltage variation is relatively small. The SVC permits to keep the voltage almost constant, while the OLTC changes the voltage due to tap changes; no significant effects are due to distributed generators. Node #10 is located in the middle of the feeder; in this case, the voltage control performed by the centralized SVC or distributed devices is similar. As in the other cases, the OLTC has the worst performance.

Future work will explore other possible solutions for voltage control in which both centralized and distributed devices do coexist. The performance of new proposed cooperation techniques in old systems without communication will be compared with smart grid solutions, in which distributed and centralized devices can communicate with each other. Regarding the use of an OLTC, it will be studied more in details, varying the number of tap changes and considering the related O&M costs.

REFERENCES

[1] International Energy Agency (IEA), "Trends 2016 in Photovoltaic applications," 2016, Online: http://www.iea-pvps.org/index.php?id=32

[2] International Energy Agency (IEA), "IEA-PVPS Task 1 - A Snapshot of Global PV Markets 2014," 2014, Online: http://www.iea-pvps.org/index.php?id=32

[3] F. Spertino, P. Di Leo, F. Corona and F. Papandrea, "Inverters for grid connection of photovoltaic systems and power quality: Case studies," 3rd IEEE International Symposium on Power Electronics for Distributed Generation Systems (PEDG), Aalborg, 2012, pp. 564-569.

[4] Standard EN 50160, "Voltage characteristics of electricity supplied by public distribution systems".

[5] W. Heckmann, D. Geibel, T. Degner, J. Ostergaard, "Application of MV/LV Transformers with OLTC for Increasing the PV Hosting Capacity Of LV Grids," 31st European Photovoltaic Solar Energy Conference and Exhibition - Hamburg, Germany, 2015, pp.1659-1662

[6] D. A. Sarmiento, P. P. Vergara, L. C. P. da Silva and M. C. de Almeida, "Increasing the PV hosting capacity with OLTC technology and PV VAr absorption in a MV/LV rural Brazilian distribution system," 17th International Conference on Harmonics and Quality of Power (ICHQP), Belo Horizonte, 2016, pp. 395-399

[7] M. Nijhuis, M. Gibescu and J. F. G. Cobben, "Incorporation of on-load tap changer transformers in low-voltage network planning," IEEE PES Innovative Smart Grid Technologies Conference Europe (ISGT-Europe), Ljubljana, 2016, pp. 1-6.

[8] K. Rauma, F. Cadoux, N. Hadj-Saïd, A. Dufournet, C. Baudot and G. Roupioz, "Assessment of the MV/LV on-load tap changer technology as a way to increase LV hosting capacity for photovoltaic power generators," CIRED Workshop 2016, Helsinki, 2016, pp. 1-4.

[9] B. Kanna and S. N. Singh, "Predictive short-term ORPD in large wind farms for minimization of losses and OLTC tap movements," National Power Systems Conference (NPSC), Bhubaneswar, India, 2016, pp. 1-6.

[10] E. Z. Abdel-Aziz, J. Ishaq, A. M. Al-Khulayfi and Y. T. Fawzy, "Voltage stability improvement in transmission network embedded with photovoltaic systems," IEEE International Energy Conference (ENERGYCON), Leuven, 2016, pp. 1-7.

[11] CEI 0-21, Reference technical rules for the connection of active and passive users to the LV electrical Utilities, 2016 CEI, Online: http://ceiweb.it/doc/norme/14829.pdf

[12] G. M. Tina and G. Celsa, "Active and reactive power regulation in grid-connected PV systems," 50th International Universities Power Engineering Conference (UPEC), Stoke on Trent, 2015, pp. 1-6.

[13] F. Spertino, J. Ahmad, G. Chicco, A. Ciocia and P. Di Leo, "Matching between electric generation and load: Hybrid PV-wind system and tertiary-sector users," 50th International Universities Power Engineering Conference (UPEC), Stoke on Trent, 2015, pp. 1-6.

[14] F. Spertino, A. Ciocia, P. Di Leo, R. Tommasini and I. Berardone, M. Corrado, A. Infuso, M. Paggi, "A power and energy procedure in operating photovoltaic systems to quantify the losses according to the causes," Solar Energy, vol. 118, pp. 313-326, 2015.

[15] A. Mazza, G. Chicco, A. Russo and E.O. Virjoghe, "Multi-Objective Distribution Network Reconfiguration Based on Pareto Front Ranking", Intelligent Industrial Systems, vol. 2, no. 4, pp. 287–302, 2016.

[16] J. Kennedy and R. Eberhart, "Particle Swarm Optimization", Proceedings of the IEEE International Conference on Neural Networks, Perth, vol. 4, pp. 1942–1948, 1995.